CrossMark

Dexamethasone Alters the Appetite Regulation via Induction of Hypothalamic Insulin Resistance in Rat Brain

Ragitha Chruvattil[1] · Shreya Banerjee[1] · Sarmi Nath[1] · Jatin Machhi[2] ·
Gitika Kharkwal[1,3] · Mange Ram Yadav[2] · Sarita Gupta[1]

Abstract Elevated levels of glucocorticoid, a steroid hormone released in response to stress, have been implicated in the pathophysiology of diabetes, which is now known to extend its effect on brain functions. Hence, we aimed to investigate the status of brain insulin signaling in response to dexamethasone (a synthetic glucocorticoid) treatment in female Charles Foster rat. This model exhibited pronounced hyperinsulinemia and glucose intolerance with loss in appetite and body weight. Immunoblotting of insulin receptor (INSR)-PI3kinase-AKT demonstrated reduced insulin signaling in hypothalamus but no change in hippocampus, cortex, and cerebellum in dexamethasone-treated rats as compared to vehicle-treated rats, signifying the diversity of distribution and function of insulin in different brain regions. These results also correlated with appetite change, a key function governed by hypothalamus. Hence, we further explored the hypothalamic feeding circuit and found altered levels of neuropeptide genes (*Agrp*, *Npy*, *Pomc*) and candidate nutrient sensors (GLUT1, SirT1, and PPARγ). There was also a considerable reduction in glycogen content and appetite-regulating neurotransmitters (GABA, glutamate, dopamine) in dexamethasone-treated rats. Thus, concluding that dexamethasone not only induces peripheral insulin resistance but also impairs hypothalamic function of appetite regulation via the interwoven cascade of insulin signaling, neurotransmitters, and neuropeptides.

Highlights • Hypothalamus is the prime region for onset of dexamethasone-induced brain insulin resistance.
• Dexamethasone modulates the hypothalamic appetite-regulating circuitry.
• Decision of appetite depends on cross talk of insulin signaling, glucocorticoid levels, nutrient sensors, neurotransmitters, and neuropeptides in hypothalamus.

Electronic supplementary material The online version of this article (doi:10.1007/s12035-016-0251-2) contains supplementary material, which is available to authorized users.

✉ Sarita Gupta
   sglmescrl@gmail.com

[1] Department of Biochemistry, Faculty of Science, The Maharaja Sayajirao University of Baroda, Vadodara, Gujarat 390002, India

[2] Faculty of Pharmacy, The Maharaja Sayajirao University of Baroda, Vadodara, Gujarat 390001, India

[3] Present address: ICMR Headquarters, Ansari Nagar, New Delhi Delhi-110029, India

Introduction

Brain insulin signaling mediates several metabolic, neurotrophic, neuromodulatory, and neuroendocrine actions [1, 2]. Any insult leading to alterations in brain insulin signaling (via decreased insulin levels or brain insulin resistance) can culminate into structural, neurophysiological, and neuropsychological defects [3–5]. One of the most important clinical manifestation, which can cause peripheral [6] as well as brain insulin resistance [7], is the elevated level of circulating glucocorticoid. The rise in circulating glucocorticoid level can be caused because of physiological condition of stress, obesity, adrenal hypertrophy, obsessive-compulsive disorder, anorexia nervosa, or exogenous steroid (dexamethasone) treatment [8]. Insulin and glucocorticoid have antagonist effects and via activating their respective receptors in brain, result into plasticity of several brain functions such as appetite regulation, learning and memory, and mood disorders. Insulin is

 Springer

known to mediate these effects by modulating the levels as well as actions of neuropeptides, e.g., NPY and POMC; neurotransmitter, e.g., GABA; and nutrient sensors, e.g., Gluts and SirT1 [9–12].

One of the most important aspects of insulin signaling in brain is maintenance of energy homeostasis by hypothalamus. Several attempts have been made to explore new insights in the deregulation of hypothalamic insulin signaling during diabetes and stress. Intracerebroventricular (i.c.v) injection of insulin is known to suppress food intake, which can be reverted by administration of either of the two PI3K inhibitors—wortmannin and LY294002, supporting insulin-mediated PI3K-dependent mechanism in hypothalamus [13]. There are appetite-stimulating neurons in the hypothalamus that co-express neuropeptide Y (NPY) and agouti-related protein (AgRP), which are insulin responsive, and their expression is inhibited by insulin [14]. Adjacent to these cells are neurons that express pro-opiomelanocortin (POMC), the polypeptide precursor from which melanocortins such as α-melanocyte-stimulating hormone (α-MSH) are derived that activate neuronal melanocortin receptors, thereby decreasing food intake and favoring weight loss. POMC neurons are stimulated by insulin but inhibited by neighboring NPY/AgRP neurons [15]. Similarly, to investigate the effect of glucocorticoids, in vivo rodent models have been established using dexamethasone, a synthetic glucocorticoid [16]. Reports have demonstrated that in rodent models, dexamethasone treatment combined with high-fat diet lead to obesity [17]; however, treatment with dexamethasone alone significantly reduces body weight in spite of elevated expression of hypothalamic NPY [18, 19]. Thus, appropriate mechanism involving hypothalamic regulation of appetite loss is not well understood in this model.

Apart from accounting for the change in neuropeptide levels, insulin and glucocorticoid are known to play an important role as neuromodulators and are involved in synthesis, release, and degradation of neurotransmitters [20, 21]. Neurotransmitters also host for the feeding behavior, and most of the synaptic activities in the hypothalamus are dependent on the amino acids glutamate and γ-aminobutyric acid (GABA) [22]. Also, among appetite-related brain messengers, dopamine is an essential neurotransmitter for feeding, where the absence of dopamine causes an inability to initiate feeding [23].

Since substantial research has examined the effect of fructose/high-fat diet on brain insulin resistance [24–27], we aimed to explore the impact of excess glucocorticoid using dexamethasone-treated rat model on insulin signaling in brain. Furthermore, the status of the hypothalamic appetite-regulating machinery has been explored in the current study, which has not received much attention in spite of the frequent observation of weight loss and reduced appetite in this model.

Materials and Methods

Chemicals

Dexamethasone was procured from Zydus Alidac. Chemicals for western blotting was procured from Sigma-Aldrich and Sisco Research Lab (SRL).

Experimental Animals

Charles Foster rats are inbred strains of albino rats maintained in Animal House Facility, Department of Biochemistry, since 50 years for research purpose. In the current study, virgin female rats weighing 180–220 g were used (Note that the only purpose of using female rats in the current study was that we observed a profound decrease in body weight when analyzing the effect of insulin resistance on ovarian cells in dexamethasone-induced diabetic female rat model [28]. Hence, dose and duration of dexamethasone as well as phenotypic outcome in female rats were already well defined in the lab.) Rats were housed at Animal House Facility, Department of Biochemistry, with ad libitum access to water and chow (chow was procured from Pranav Agro Industries Ltd., Pune, India) in a well-ventilated animal unit (26–28 °C, humidity 60%, 12-h light-dark cycle). Care and procedures adopted for the present investigation were in accordance with the approval of the CPCSEA or Institutional Animal Ethics Committee (938/a/06/CPCSEA). Four rats per group was kept for assessment of protein expression study, gene expression study, glycogen content, and neurotransmitter estimation. The groups were

- Vehicle control (control): normal saline (N. saline) was injected subcutaneously (s.c.) for 28 days.
- Dexamethasone (dexa)-treated group: subcutaneous (s.c.) injection of 3 mg dexamethasone/kg body weight/day for 28 days [28].

Rats were housed individually while body weight and food intake were monitored at a regular interval during the treatment period. The food intake in grams per 24 h was monitored at a regular interval of 3 days. A known amount of rat food pellet (in grams) was given to the experimental animals, and the food intake (g/day) was calculated as [(food pellet given at 0 h) − (food pellet left uneaten after 24 h)]. On 28th day, rats were kept for overnight fasting, and validation of insulin resistance was done on 29th day by estimating fasting serum glucose and insulin levels. After validation of peripheral insulin resistance, rats had ad libitum access to chow and water and were sacrificed in the proestrus stage.

Confirmation of Insulin Resistance and Oral Glucose Tolerance Test

Standard oral glucose tolerance test was performed after 28 days of treatment period. After 12 h of overnight fasting, blood was collected from retro-orbital sinus for glucose and insulin measurement, followed by oral administration of 2-g/kg body weight glucose. After glucose load, blood collection was performed at 0, 30, 60, 90, and 120 min for oral glucose tolerance test (OGTT). The blood was allowed to clot at room temperature for 30 min followed by centrifugation at 2000g for 10 min for serum separation. Glucose was estimated from serum using glucose oxidase and peroxidase (GOD POD) method as per the manufacturer's instructions (Reckon). Insulin levels were determined from fasting serum using Rat Insulin ELISA Kit according to the manufacturer's protocol (Mercodia, Germany). The fasting insulin resistance index (FIRI), a measure of the insulin sensitivity, was calculated according to the following formula: FIRI = [fasting serum insulin (μIU/mL) × fasting serum glucose (mmol/L)]/25 [29].

Serum Corticosterone Estimation

Corticosterone levels were estimated from serum separated from blood collected during 7–8 p.m. during proestrus stage. Briefly, corticosterone was extracted from serum using 1 mL dichloromethane (Sigma 270997). After centrifugation, aqueous phase was removed and given brief alkaline wash with 1 mL 0.01 N NaOH followed by centifugation and removal of alkaline phase. Of the 30 N sulfuric acid, 800 μL was added to the solvent phase, vortexed for 10–15 s, and after centrifugation removed the upper solvent layer. Acidic corticosterone-containing phase was incubated at room temperature for 30 min (in dark), and the fluorescence of the sample was determined with an excitation wavelength of 472 nm and emission wavelength of 523 nm using Fluorescence Spectrophotometer (Hitachi F-7000). The fluorescence intensity was calculated from the standard curve prepared in charcoal-stripped serum, after correction for the low reading obtained with the blank carried through the same procedure [30, 31].

Protein Expression Study

Cortex, cerebellum, hippocampus, and hypothalamus were dissected out as per the rat brain dissection manual [32, 33], homogenized in buffer (50 mM Tris-HCl, pH 7.4, 150 mM NaCl, 0.5% Triton X-100, 1 mM EDTA, protease inhibitor cocktail), and stored in aliquots at −80 °C. Tissue homogenates were centrifuged (14,000g), and aliquots of the clear extract were boiled in Laemmli SDS sample buffer. Of the total protein, 40 μg was resolved on 12% SDS-PAGE Tris-glycine gels and transferred to nitrocellulose membrane. Non-specific binding was blocked by incubating the membranes in

5% BSA and 0.1% Tween in Tris-buffered saline (TBS; pH 7.4) for 1 h at room temperature. The blots were subsequently incubated with primary antibodies against INSRβ, phospho-INSRβ (Y-1361), PI3 kinase, total AKT, phospho-AKT (S-473), total AMPKα, phospho-AMPKα (T-172), SirT1, GLUT1, PPARα, PPARγ, and β actin overnight at 4 °C, with gentle agitation. Blots were washed with TBS containing 0.1% Tween (TBS-T) (4 × 15 min) and then incubated with respective secondary antibodies conjugated with HRP for 2 h at room temperature with gentle agitation. For details of antibody, please refer to Table 1. After four washes with TBS-T and one wash with TBS, specific bands of immunoreactive proteins were visualized using enhanced chemiluminescence (ECL) reagent (Millipore) in Chemidoc (Alliance model 4.7). Densitometric analysis of the protein bands was calculated by ImageJ software. Intensities of target proteins were normalized with that of loading control, i.e., β actin probed on the same blot. The ratio of phosphorylated proteins to that of total protein was calculated after normalization to β actin.

Gene Expression Study

Total RNA was isolated from the hypothalamus using TRIzol (Invitrogen). Total RNA was quantified and messenger RNA (mRNA) samples were reverse-transcribed into cDNAs using High-Capacity cDNA Synthesis Kit (Invitrogen) according to the manufacturer's instructions. Gene expression of corticotropin-releasing hormone (*Crh*), neuropeptide Y (*Npy*), agouti-related peptide (*Agrp*), propiomelanocortin (*Pomc*), leptin receptor (*Obrb*), melanocortin 4 receptor (*Mc4r*), monocarboxylate transporter 1 (*Slc16a1*), monocarboxylate transporter 4 (*Slc16a3*), and glial-specific glutamate transporters (*Glt1* and *Glast*) were measured via real-time RT-PCR technique using SYBR Green chemistry (7500 Applied Biosystem Real-Time PCR) (refer to Table 2 for details of primer sequence). The Ct values of target genes were normalized to that of *Actb* levels to calculate ΔCt. The graph was plotted as relative fold change of expression of target genes which was quantified as $2^{-(\Delta\Delta Ct)}$, where ΔΔCt was ΔCt (target gene expression in test group) − ΔCt (target gene expression in control group).

Neurotransmitter Estimation

Glutamate and GABA Estimation

The hypothalamus was dissected out, rinsed with ice cold PBS, weighed, and homogenized in 10% of 0.17 M perchloric acid. The amino acid standard was prepared by spiking known amount of mixed standards (10, 20, 40, 80, and 160 ng/mL of each glutamate and GABA) in pooled brain homogenate. The homogenates were kept on ice for at least 30 min for complete protein precipitation. The homogenate was then centrifuged at

Table 1 List of antibodies used in western blotting with their dilutions

Antibody type	Antigen	Name provided by supplier	Supplier details	Dilution
Primary monoclonal	β actin	Anti-β actin monoclonal antibody	Thermo Scientific (catalog no. MA1–91399)	1:5000
Primary polyclonal	Insulin receptor β	Polyclonal rabbit anti-CD220 (insulin receptor β)	BD Transduction Laboratories (catalog no. 611277)	1:1000
Primary polyclonal	Phospho-insulin receptor (Y-1361)	Phospho-IR pTyr1361 antibody	Thermo Fisher (catalog no. PA5–35787)	1:1000
Primary	GLUT1	Anti-GLUT1, C-terminal antibody	Sigma-Aldrich (catalog no. SAB 4502803)	1:1000
Primary monoclonal	PPARγ	PPARγ (C26H12) rabbit mAb	Cell Signaling Technology (catalog no. 2435)	1:1000
Primary monoclonal	PPARα	Monoclonal anti-peroxisome proliferator-activated receptor α	Sigma (catalog no. P 0869)	1:1000
Primary monoclonal	PI3 kinase p85	PI3 kinase p85 (19H8) rabbit mAb	Cell Signaling Technology (catalog no. 4257)	1:1000
Primary monoclonal	Total Akt	Akt (pan) (C67E7) rabbit mAb	Cell Signaling Technology (catalog no. 4691)	1:1000
Primary monoclonal	Phospho-Akt	Phospho-Akt (Ser473) (D9E) XP rabbit mAb	Cell Signaling Technology (catalog no. 4060)	1:1000
Primary monoclonal	SirT1	SirT1 (D1D7) rabbit mAb	Cell Signaling Technology (catalog no. 9475)	1:1000
Primary monoclonal	AMPKα	AMPKα (D63G4) rabbit mAb	Cell Signaling Technology (catalog no. 5832)	1:1000
Primary monoclonal	Phospho-AMPKα (Thr172)	Phospho-AMPKα (Thr172) (40H9) rabbit mAb	Cell Signaling Technology (catalog no. 2535)	1:1000
Secondary	Anti-mouse IgG	Goat anti-mouse poly-HRP	Thermo Scientific (catalog no. 32230)	1:2500
Secondary	Anti-rabbit IgG	Goat anti-rabbit poly-HRP	Thermo Scientific (catalog no. 32260)	1:2500

4 °C for 20 min at 12,000g. After centrifugation, supernatants were separated and either immediately analyzed or stored at −70 °C until assayed. The amount of glutamate and GABA was assessed by RP-HPLC coupled with electrochemical detector (model no. Waters 2465; Waters Corporation, Milford, USA). Estimation was performed according to the previously described method with minor modifications in the derivatization step [34]. Briefly, a Sunfire® C18 column

Table 2 List of primers with their sequences used in real time PCR

Gene	Forward primer 5′-3′	Reverse primer 5′-3′	Product length	Accession
Npy	AAT CAG TGT CTC AGG GCT GGA T	CCG CTC TGC GAC ACT ACA TC	73	NM_012614.2
Pomc	AAG AGC AGT GAC TAA GAGAGG CCA	ACG TCT ATG GAG GTC TGA AGC AGG	152	NM_139326.2
Agrp	CGG AGG TGC TAG ATC CAC AGA	AGG ACT CGT GCA GCC TTA CAC	66	NM_033650.1
Crh	CCA GGG CAG AGC AGT TAG CT	CAA GCG CAA CAT TTC ATT TCC	80	NM_031019.1
Cart	GCC AAG TCC CCA TGT GTG AC	CAC CCC TTC ACA AGC ACT TCA	128	NM_017110.1
Obrb	GCATGCAGAATCAG TGATATTTGG	CAAGCTGTATCGAC ACTGATTTCTTC	81	NM_012596.1
Mc4r	ACG CGC TCC AGT ACC ATA AC	AAA GAA CGC CCG ATA CTG TG	112	NM_013099.2
Glt1	CCGAGCTGGACACCATTGA	CGGACTGCGTCTTGGTCAT	68	NM_017215.2
Glast	CCATCCAGGCCAACGAAA	GCCGAAGCACATGGAGAA	158	NM_019225.2
Slc16a1	TGGAATGTTGTCCT GTCCTCCTGG	TCCTCCGCTTTCTGTTCTTT GGC	178	NM_012716.2
Slc16a3	TTCTCCAGTGCCAT TGGTCTCGTG	CCCGCCAGGATGAA CACATACTTG	122	NM_030834.1
Actb	CTTCTGACCCATAC CCACCA	ATGGATGACGATAT CGCTGC	150	NM_031144.3

(4.6 × 150 mm, particle size 5 μm) was used, and separation was carried out using mobile phase containing a solution of 0.1 M monosodium phosphate, and 0.5 mM EDTA, 25% (v/v) methanol; pH was adjusted to 4.5, at a flow rate of 1.2 mL/min and an operating potential of 0.85 V. The solution was made in degassed deionized water. The derivatization reagent mixture consisted of 37 mM orthopthaldehyde (OPA), 50 mM sodium sulfite, 90 mM tetraborate buffer (which was set to pH 10.4 with sodium hydroxide, prior to addition of OPA), and 5% methanol [35]. For preparation of standard calibration curve, 20 μL of derivatizing reagent was mixed with 1 mL of amino acid standard for 10 min. After incubation, 20 μL of sample was injected in HPLC. For sample analysis, 20 μL of the supernatant was mixed with 0.4 μL of the derivatizing reagent and incubated at room temperature for 10 min. Of the mixed supernatant, 20 μL was injected in HPLC. The standard curves were used to quantify the amount of glutamate and GABA in each sample by calculating the area under curve (AUC).

Dopamine Estimation

For dopamine estimation, sample preparation was same as that for glutamate and GABA estimation. Of the deproteinized sample, 20 μL was injected in HPLC with Sunfire® C18 column (4.6 × 150 mm, particle size 5 μm), and separation was carried out using mobile phase containing methanol (15% v/v) in a solution (pH 4.2) of 32 mM citric acid, 12.5 mM disodium hydrogen orthophosphate, 0.5 mM octyl sodium sulfate, 0.5 mM EDTA, and 2 mM KCl, at a flow rate of 1.2 mL/min, an operating pressure of 3000 psi, and an operating potential of 0.61 V. The internal standard curves were prepared by spiking known amounts of mixed standard (10, 20, 40, 80, and 160 ng/mL of dopamine (DA)) in 1 mL of pooled brain homogenates. The standard curves were used to quantify the amount of DA in each sample by calculating the AUC.

Glycogen Content

Glycogen content was measured according to the periodic Schiff method [36] with slight modifications. In brief, 15 mg of hypothalamus was boiled in 30% KOH, followed by the precipitation with absolute ethanol. The pellet was resuspended in 0.2 M NaCl. Of the sample, 200 μL was incubated at 37 °C for 2 h with 20 μL of 50% of periodic solution in 7% acetic acid. After periodate oxidation, 20 μL of Schiff's reagent was added and incubated for 30 min for the color development. The absorbance was taken at 555 nm and the concentration was calculated as per the standard plot of glycogen (range 0–400 μg/mL) normalized to tissue weight.

Statistical Analysis

Results are presented as mean ± SEM of the indicated number of experiments. Statistical significance was determined using the unpaired Student's t test or two-way analysis of variance followed by Bonferroni posttest using GraphPad Prism 3 software. P value less than 0.05 was considered to be statistically significant.

Results

Confirmation of Peripheral Insulin Resistance in Dexamethasone-Treated Rats

The alterations in food intake and body weight during the length of 24 h at a regular interval of 3 days was monitored in rats treated with vehicle or dexamethasone for 28 days. A statistically significant reduction in body weight (Fig. 1a) with a change in food intake (Fig. 1b) was observed in rats following dexamethasone treatment for 28 days as compared to vehicle-treated control rats (control). At the end of the treatment period, dexamethasone-treated group demonstrated mild fasting hyperglycemia with significant intolerance to oral glucose as shown in Fig. 1c. The fasting glucose levels, insulin levels, and FIRI positively correlated with an insulin-resistant phenotype in dexamethasone-treated rats as shown in Table 3. Chronic treatment with dexamethasone suppressed the endogeneous corticosterone level as shown in Table 3. Thus, dexamethasone treatment resulted in reduced appetite, body weight, and endogenous corticosterone levels along with a marked rise in glucose intolerane and FIRI.

Dexamethasone Treatment Impairs Insulin Signaling in Hypothalamus with No Change in Hippocampus, Cortex, and Cerebellum in Rats

It is known that binding of insulin to its plasma membrane receptor (INSR) elicits various intracellular signaling pathways, which mediate the effects of insulin [37]. To determine whether dexamethasone treatment affects insulin signaling in brain, we examined the protein levels of phospho-INSRβ (Y-1361), total INSRβ, PI3 kinase, phospho-AKT (S-473), and total AKT in the hypothalamus (Fig. 2a), hippocampus (Fig. 2b), cerebral cortex (Fig. 2c), and cerebellum (Fig. 2d) of rats treated with vehicle or dexamethasone for 28 days. We found a regional difference in insulin signaling in brain following dexamethasone treatment. Specifically, dexamethasone treatment reduced insulin signaling in the hypothalamus (Fig. 2a) as shown by the INSRβ activity, PI3 kinase, and AKT activity. However, no significant change was observed in hippocampus (Fig. 2b), cerebral cortex (Fig. 2c), and cerebellum (Fig. 2d) in dexamethasone-treated rats as compared to
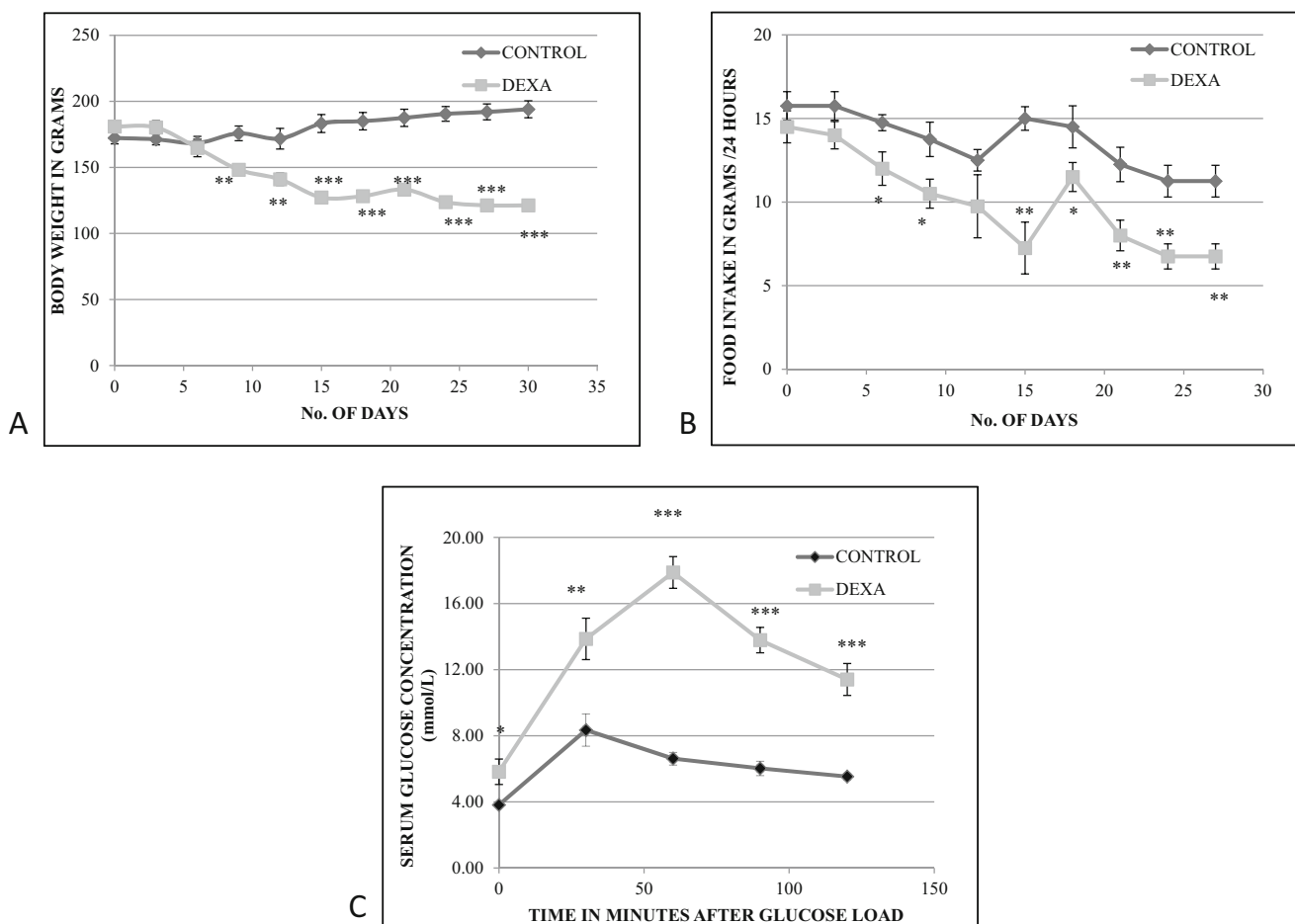
Fig. 1 Assessment of body weight, food intake, and oral glucose tolerance. Body weight (in grams) (**a**) and food intake (in grams/24 h) (**b**) were monitored throughout the treatment period in dexamethasone (dexa)-treated rats and vehicle control (control) rats. Oral glucose tolerance test (OGTT) (**c**) after 28 days of treatment demonstrated that there was glucose intolerance in dexa-treated rats as compared to vehicle control (control). Data presented as mean ± SEM of $n = 6$ for control and dexa group. *p value <0.05 as compared to control; **p value <0.01 as compared to control; ***p value <0.001 as compared to control. Comparisons were performed by two-way analysis of variance, followed by pairwise Bonferroni posttest using GraphPad Prism 3 software

vehicle control (also refer to supplementary result Fig. S1). Since hypothalamic insulin signaling as well as feeding behavior were severely affected, we further carried out in-depth analysis of candidate players involved in hypothalamic appetite regulation.

Dexamethasone Alters Gene Expression of Hypothalamic Neuropeptides and Neurotransmitters in Rats

Hypothalamic appetite regulation is mediated by aneroxic and orexic neuropeptides, which are modulated in response to peripheral signals like insulin, leptin, and glucocorticoids. The gene expression of *Obrb* (Fig. 3a), which relays the signal of leptin to modulate the expression of neuropeptides, remained unchanged because of dexamethasone treatment. However, there was a remarkable upregulation of *Agrp* (Fig. 3b) and *Npy* (Fig. 3c), which acts as orexic signals, whereas there was a downregulation of *Pomc* (Fig. 3d) and *Mc4r* (Fig. 3e), which are the an orexic signals. There was no significant

change in the expression of *Cart* (Fig. 3f) and *Crh* (Fig. 3g) in dexamethasone-treated group as compared to vehicle control.

Different lines of investigations suggested that disturbances of eating behavior are associated with hypothalamic neurotransmission. Hence, the level of neurotransmitters was analyzed, and results demonstrated that there was a significant decrease in the level of glutamate (Fig. 3h), GABA (Fig. 3i), and dopamine (Fig. 3j) in hypothalamus of dexamethasone-treated group as compared to vehicle control.

Dexamethasone Treatment Alters the Level of Candidate Nutrient Sensors in Hypothalamus in Rats

Hypothalamic nutrient sensors play an important role in maintaining whole-body energy homeostasis by integrating information on energy status; hence, we analyzed the candidate nutrient sensors in hypothalamus. Glucose transporter-1 (GLUT1) in the hypothalamic glial cells mediates glucose

Table 3 Biochemical parameters of dexamethasone-treated rats (dexa) as compared to control rats

	Control	Dexa
Fasting serum insulin (μIU/mL)	4.59 ± 1.71	58.21 ± 9.9**
Fasting serum glucose (mmol/L)	2.55 ± 0.86	3.56± 0.9*
Fasting insulin resistance index (FIRI)	0.4 ± 0.27	8.3 ± 2.7**
Serum corticosterone (ng/mL)	314.52 ± 16.70	167.81 ± 21.47**

Data presented as mean ± SEM of $n = 4–6$ for control and dexa group

*p value <0.05 as compared to control

**p value <0.001 as compared to control

sensing, while PPARs are widely known as metabolic sensors for lipids. We found that there was reduction in the protein expression of brain glucose transporter, i.e., GLUT1 (Fig. 4b), and a key regulator of energy homeostasis, i.e., PPARγ (Fig. 4d) with no change in PPARα (Fig. 4c) in hypothalamus of dexamethasone-treated rats as compared to vehicle control. Similarly, SirT1 and AMPK are also critical nutrient-sensing pathways known to be associated with insulin signaling. The results demonstrated significant downregulation in the SirT1 protein levels (Fig. 4e) with no change in the activation of AMPK signaling (Fig. 4f) in hypothalamus of dexamethasone-treated rats as compared to vehicle control.

Dexamethasone Treatment Reduces Hypothalamic Glycogen Content in Rats

Glycogen granules are the vital energy stores and are known to be mobilized during high-energy requirement. Also, insulin and dexamethasone regulate the glycogen homeostasis, i.e., its synthesis and breakdown. We found that there was drastic decrease in hypothalamic glycogen content in dexamethasone group as compared to control group (Fig. 5).

Dexamethasone Treatment Downregulates Gene Expression of Hypothalamic Glutamate Transporter (GLT1) with No Change in Monocarboxylate Transporters in Rats

The role of astrocyte-specific glutamate transporter are very crucial in maintaining the glutamate homeostasis and are known to be altered in diseased condition. The gene expression study demonstrated that there was a significant decrease in the levels of *Glt1* (Fig. 6b) with no change in *Glast* (Fig. 6a), *Slc16a1* (Fig. 6c), and *Slc16a3* (Fig. 6d) in dexamethasone-treated group as compared to vehicle control.
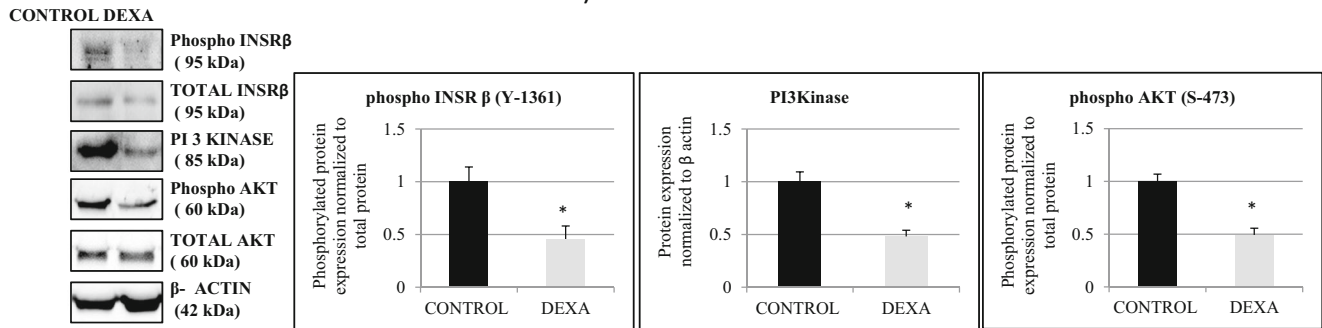
Discussion

Brain was initially thought to be an insulin-independent organ, which now has begun to be considered as an insulin-responsive organ with the advent of the fact that insulin from blood can enter brain, where it can activate its cognate receptors to modulate several functions [38]. Dexamethasone-induced, insulin-resistant model is widely used in vitro and in vivo system to examine the pathophysiology of peripheral insulin resistance [16, 39]. But, very few reports emphasized that apart from hampering insulin sensitivity in insulin-dependent peripheral tissues, dexamethasone can also downregulate insulin signaling in brain [7]. An attempt has been made in present study to understand the brain insulin resistance as well as elucidation of the links responsible for the appetite change after chronic dexamethasone treatment. Although brain appears to be protected against moderate amounts of synthetic glucocorticoids such as dexamethasone by a drug-exporting P-glycoprotein in the blood-brain barrier [40], the chronic high dose of dexamethasone as used in the current study can produce glucocorticoid receptor occupancy in the brain [41].
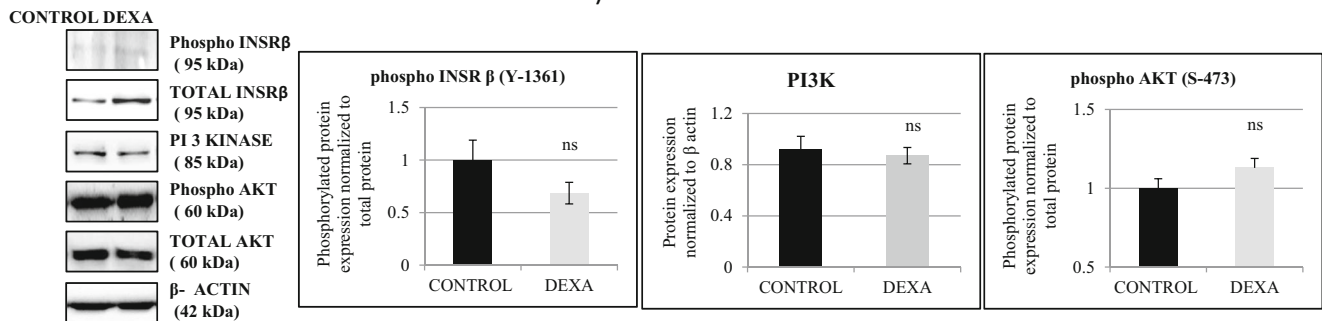
Since insulin receptors are not evenly distributed throughout the brain, regional analysis of the brain insulin signaling was assessed in dexamethasone-treated and control rats. Our foremost observation in the present study was that peripherally administered dexamethasone exerts region-specific effect on brain insulin signaling, where only hypothalamus had a prominent decrease in insulin signaling. Since hypothalamus has a leaky blood-brain barrier [42], it becomes more susceptible to peripheral hyperinsulinemia and hyperglycemia, thus speculating that persistent hyperinsulinemia might have triggered hypothalamic insulin resistance as a compensatory mechanism [43]. Also, there are glucose-sensing hypothalamic neurons which can respond to glycemic status which results in counter regulatory imbalances in response to high level of glucose or insulin resistance [44, 45]. Thus, hypothalamic insulin resistance is one of the prime events in dexamethasone-treated rats. Hypothalamic insulin receptors are crucial for the central regulation of appetite behavior, and we observed that food consumption and body weight were reduced in dexamethasone-treated rats. A frequent observation in this type of in vivo model of dexamethasone treatment has been reduction in food intake and body weight [46]; however, not much information is available on the effect of this treatment on hypothalamic regulation of feeding.

Impaired insulin signaling with an emergence of insulin resistance-like condition was evident in the hypothalamus of
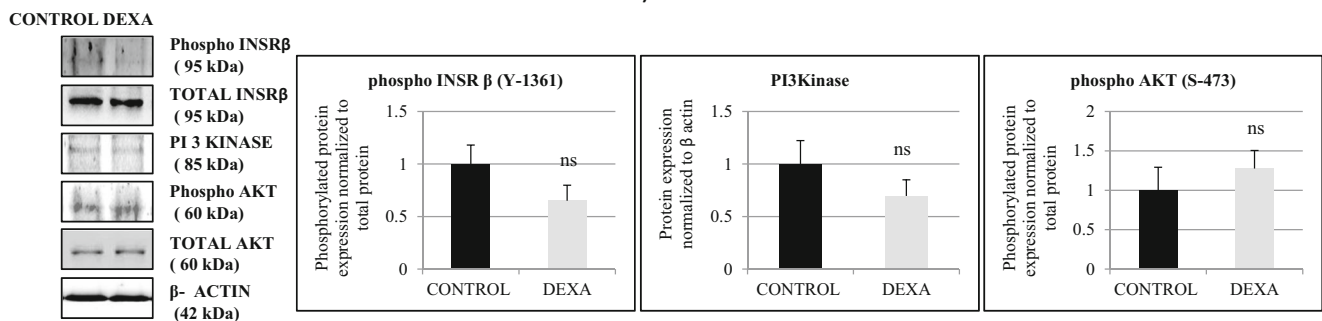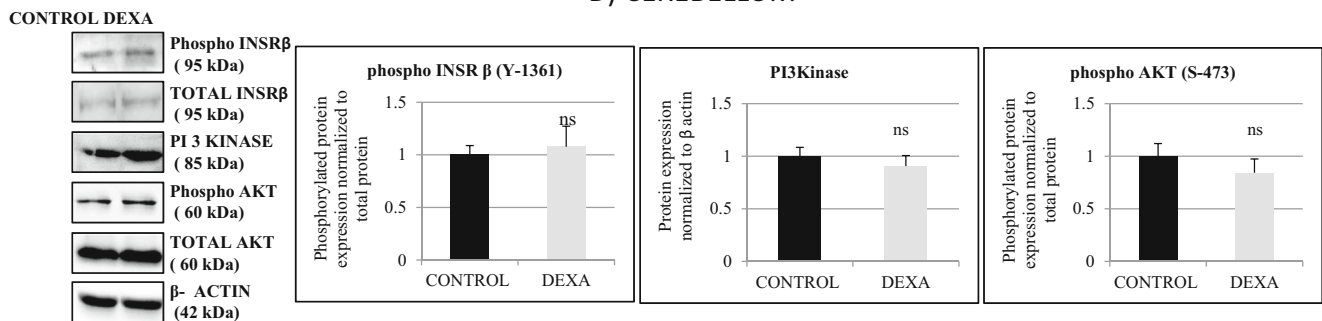
A) HYPOTHALAMUS

CONTROL DEXA

Phospho INSRβ
(95 kDa)

TOTAL INSRβ
(95 kDa)

PI 3 KINASE
(85 kDa)

Phospho AKT
(60 kDa)

TOTAL AKT
(60 kDa)

β- ACTIN
(42 kDa)

B) HIPPOCAMPUS

CONTROL DEXA

Phospho INSRβ
(95 kDa)

TOTAL INSRβ
(95 kDa)

PI 3 KINASE
(85 kDa)

Phospho AKT
(60 kDa)

TOTAL AKT
(60 kDa)

β- ACTIN
(42 kDa)

C) CORTEX

CONTROL DEXA

Phospho INSRβ
(95 kDa)

TOTAL INSRβ
(95 kDa)

PI 3 KINASE
(85 kDa)

Phospho AKT
(60 kDa)

TOTAL AKT
(60 kDa)

β- ACTIN
(42 kDa)

D) CEREBELLUM

CONTROL DEXA

Phospho INSRβ
(95 kDa)

TOTAL INSRβ
(95 kDa)

PI 3 KINASE
(85 kDa)

Phospho AKT
(60 kDa)

TOTAL AKT
(60 kDa)

β- ACTIN
(42 kDa)

dexamethasone-treated rats as compared to vehicle control rats, where there was downregulation of candidate insulin-signaling proteins. This desensitization of insulin signaling can be attributed to either direct dexamethasone treatment or dexamethasone-induced hyperinsulinemia. Contradicting the earlier reports, where hypothalamic insulin resistance can promote food intake leading to gain in body weight, dexamethasone-treated animals demonstrated decrease in

◀ **Fig. 2** Immunoblotting of insulin-signaling proteins in brain. Phospho-INSRβ Y-1361, total INSRβ, PI3 kinase, phospho-AKT S-473, and total AKT, keeping β-actin as endogenous control was done by western blotting for hypothalamus (**a**), hippocampus (**b**), cortex (**c**), and cerebellum (**d**) in control and dexamethasone (dexa) -treated rats. The *graph* represents the densitometric analysis done using ImageJ software. Significant change was observed in expression of phosho-INSRβ/total INSRβ, PI3 kinase, and phospho-AKT/total AKT in hypothalamus of dexa-treated rats as compared to vehicle control (control). No change was observed in hippocampus (**b**), cortex (**c**), and cerebellum (**d**). Data presented as mean ± SEM of $n = 3–4$ for control and dexa group. *p value <0.05 as compared to control, **p value <0.01 as compared to control, and ns p value >0.05 as compared to control as calculated by unpaired Student's t test

body weight and were lean. These results clearly demonstrated that reduced insulin-mediated PI3K-AKT activation in hypothalamus is not always associated with obesity. It is in accordance with a report where impaired PI3K activation in ventromedial hypothalamus has been shown to resist the development of obesity [47].

Insulin signaling and the glycemic status are known to modulate the expression of GLUT1 [48], which is a major glucose transporter as well as a glucose sensor in brain [49]. There was a significant reduction observed in the expression of hypothalamic GLUT1 and also in SirT1, which is another metabolic sensor of glucose, thereby affecting not only glucose uptake but also glucose sensing by hypothalamus in dexamethasone-treated rats. Glucose also acts as a receptor stimulant for brain PPARγ [50], and persistent hyperglycemia has been shown to decrease its expression in key hypothalamic regions involved in glucose homeostasis [51]. Studies with brain-specific PPARγ knockout mice demonstrates that absence of brain PPARγ results in an increase in energy expenditure and a decrease in food consumption even when fed with high-fat diet [52]. Thus, reduced PPARγ expression observed in hypothalamus of dexamethasone-treated rats in present study justifies the reduction in food intake and weight loss in this model.
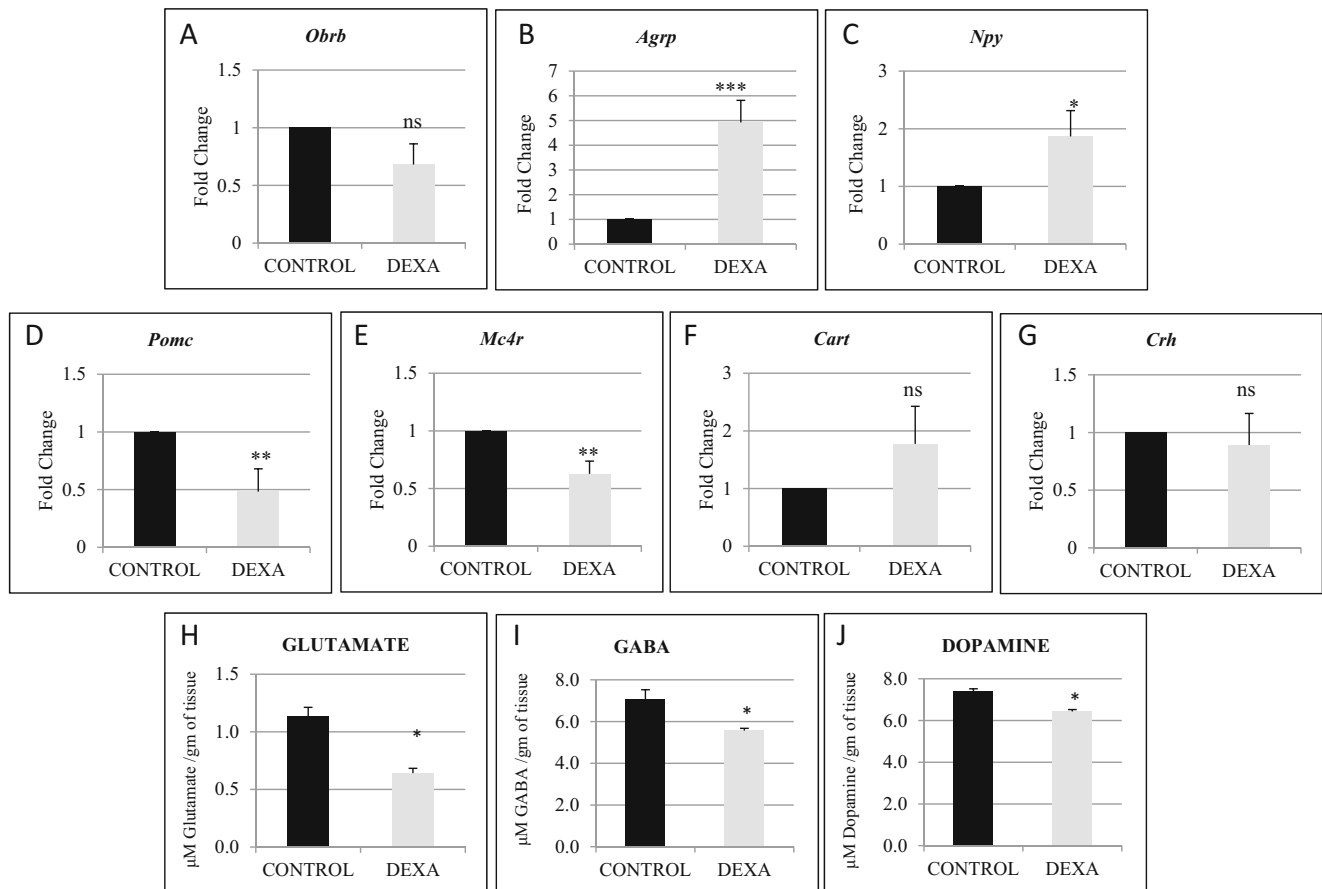

Fig. 3 Analysis of neuropeptides' gene expression and neurotransmitter levels. Quantitative real-time PCR analysis of *Obrb* (**a**), *Agrp* (**b**), *Npy* (**c**), *Pomc* (**d**), *Mc4r* (**e**), *Cart* (**f**), and *Crh* (**g**) genes from hypothalamus of vehicle control (control) and dexamethasone (dexa) rats. There was upregulation in the gene expression of *Agrp* and *Npy* and downregulation in the gene expression of *Pomc* and *Mc4r*. The threshold cycle values were normalized using *Actb* as an internal standard, and fold change ($2^{-\Delta\Delta Ct}$) was calculated from Ct values. Neurotransmitter estimation was done from the hypothalamus of control and dexa-treated rats by reverse-phase HPLC. The levels of glutamate (**h**), GABA (**i**), and dopamine (**j**) were estimated and calculated as μM of neurotransmitter per gram of tissue. Data presented as mean ± SEM of $n = 3–4$ for control and dexa group. *p value <0.05 as compared to control, *p value <0.05 as compared to control, **p value <0.01 as compared to control, and ns p value >0.05 as compared to control as calculated by unpaired Student's t test
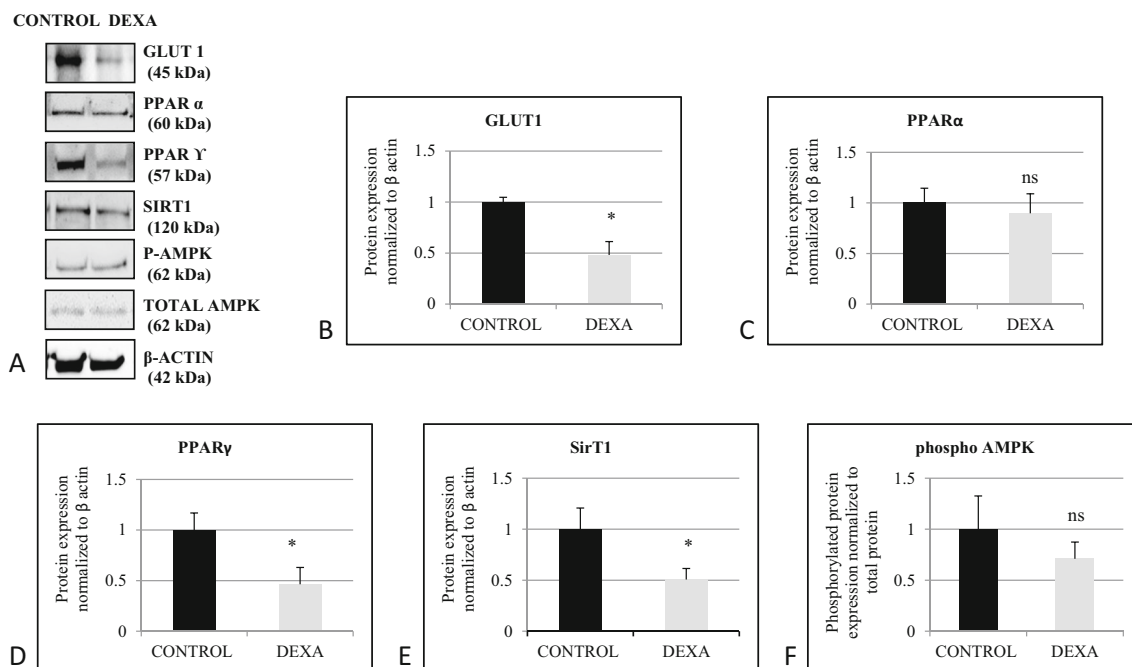
Fig. 4 Immunoblotting for hypothalamic nutrient sensors - Glucose transporter 1 (GLUT1), peroxisome proliferator-activated receptor α (PPAR α), PPARγ, SirT1, AMPKα, and phospho-AMPKα (T-172) with β actin as a reference in hypothalamus (**a**). The *graphs* represent the densitometric analysis done using ImageJ software of target proteins normalized to β actin (**b–f**). Significant change was observed in GLUT1 (**b**), PPAR γ (**d**), and SIRT1 (**e**) in hypothalamus of dexamethasone (dexa)-treated rats as compared to vehicle control (control). No change was observed in the protein expression of PPAR α (**c**) and phospho-AMPKα (Thr 172)/total AMPKα (**f**). Data presented as mean ± SEM of $n = 3$–4 for control and dexa group. $*p$ value <0.05 as compared to control and ns p value >0.05 as compared to control as calculated by unpaired Student's t test

In brain, glucose can be converted into glycogen and can be stored in the form of granules to be mobilized during energy demands [53]. Since insulin is known to stimulate astrocytic glycogen stores, reduced hypothalamic insulin signaling might be responsible for remarkable reduction in glycogen content in dexamethasone-treated rats as compared to control.
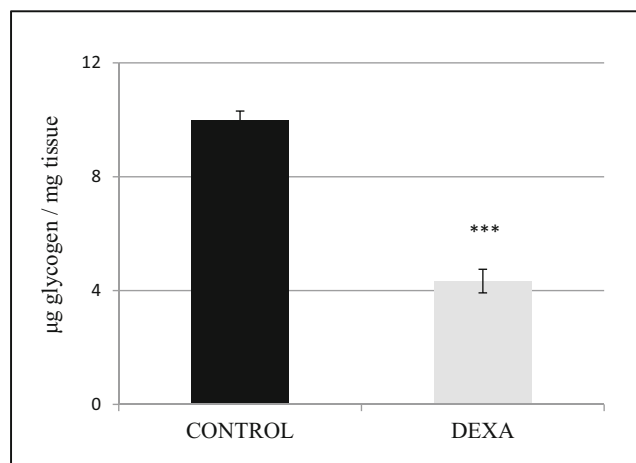

Fig. 5 Glycogen content was estimated in the hypothalamus using periodic Schiff acid microtiter assay, and a twofold decrease in the glycogen content was observed in the dexamethasone (dexa)-treated rats as compared to vehicle control (control). Data presented as mean ± SEM of $n = 4$ for control and dexa group. $***p$ value <0.001 as compared to control as calculated by unpaired Student's t test

This is comparable with the studies where diabetes is strongly associated with changes in either turnover or activity of key enzymes involved in glycogen metabolism [54, 55], highlighting that brain glycogen content plays a critical role in diabetes. There are well-established effects of dexamethasone on glycogen metabolism in peripheral organs [56], but only one report suggests that hypothalamic glycogen stores are depleted because of dexamethasone [7]. Allaman et al. [57] demonstrated that dexamethasone inhibits glycogen synthesis in astrocytes induced by nor adrenaline (NA), and this inhibition does not result from a reduced rate of glucose transport or utilization [57]. Thus, glucocorticoid-mediated hypothalamic insulin resistance causing reduced brain glycogen stores might be deleterious, since it may endanger neurons during subsequent periods of enhanced activity, as glycogen levels would be insufficient to ensure proper energy supply.

Hypothalamic insulin signaling in brain can upregulate anorexic neuropeptides such as POMC and downregulate orexigenic neuropeptides signals such as NPY and AgRP. Hence, we checked status of these neuropeptide genes having noteworthy role in feeding behavior. Although our results were in line with the existing evidences where there was upregulation of gene expression of NPY and AGRP and downregulation of POMC and MC4R as a consequence of hypothalamic insulin resistance and dexamethasone treatment, the phenotype of these rats were totally paradoxical, thus
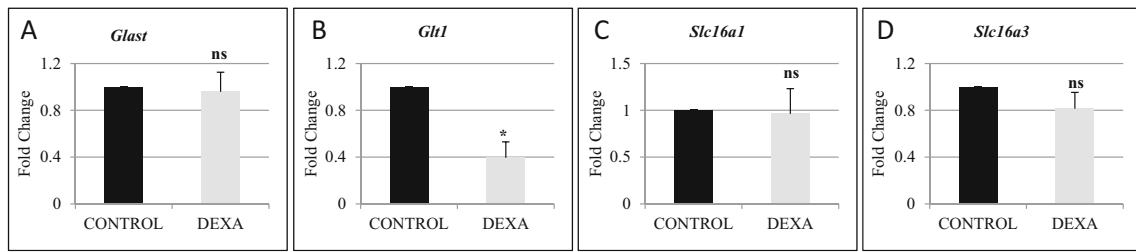
Fig. 6 Quantitative real-time PCR analysis of *Glast* (**a**), *Glt1* (**b**), *Slc16a1*(**c**), *and Slc16a3* (**d**) genes from hypothalamus of vehicle control (control) and dexamethasone (dexa)-treated rats. The threshold cycle values were normalized using *Actb* as an internal standard, and fold change ($2^{-\Delta\Delta Ct}$) was calculated from Ct values. Data presented as mean ± SEM of $n = 3–4$ for control and dexa group. *p value <0.05 as compared to control and ns p value >0.05 as compared to control as calculated by unpaired Student's t test

suggesting that hypothalamic neuropeptides alone are not the sole factor decisive for the feeding behavior.

Tong et al. proved that while both NPY and AgRP stimulate food intake when infused into the brain, the detailed analysis established that there is weight loss when AgRP-expressing cells are destroyed [58]. Also, genetic deletion of Agrp and NPY alone had little effect on feeding and body weight, and it is the GABAergic signaling that facilitates the feeding effect of NPY/AgRP at target sites in the hypothalamus [59]. These evidences indicate that the GABA is also required for the regulation of energy balance. Insulin resistance is known to decrease GAD65 mRNA expression and thus can reduce GABA level [11]. Thus, reduced GABA levels in dexamethasone-treated rats can contribute to the
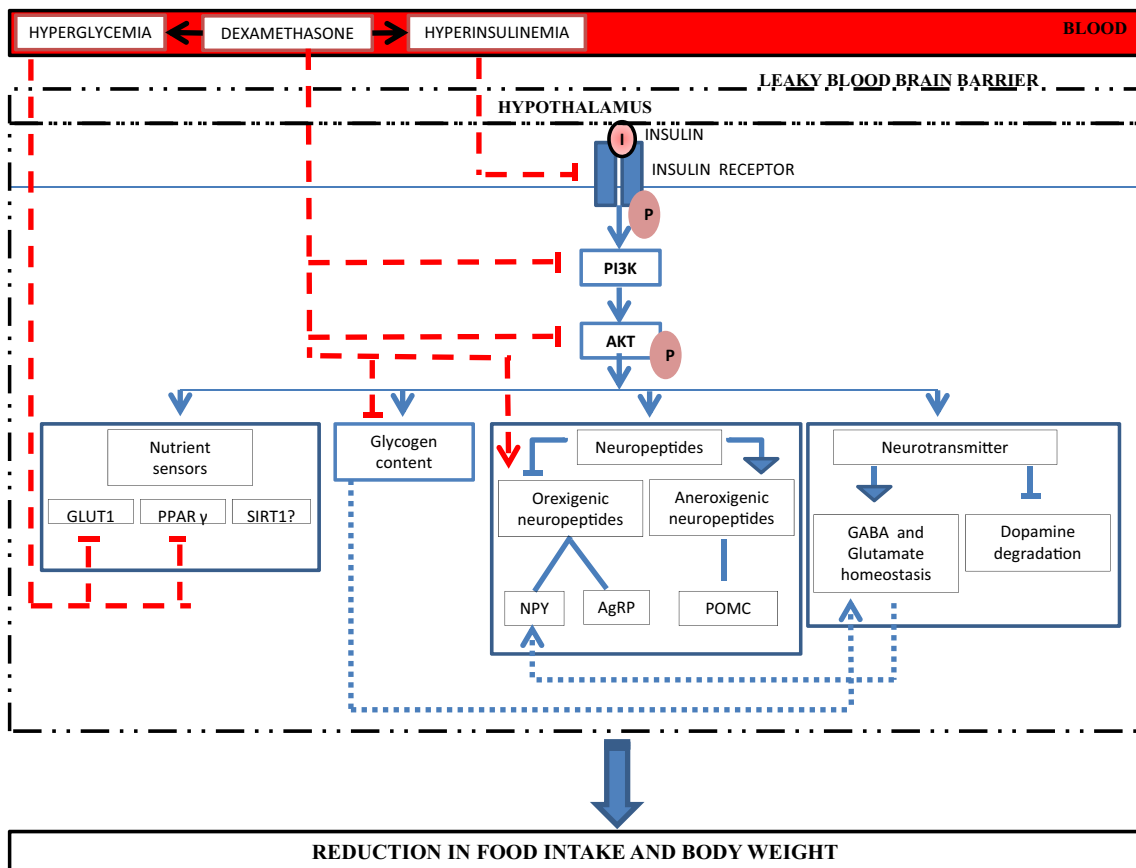

Fig. 7 Hypothalamus having leaky blood-brain barrier becomes more prone to develop insulin resistance because of dexamethasone and circulating high level of glucose as well as insulin. Hypothalamic insulin signaling can modulate several components (as shown by *bold lines*) for regulating appetite. Dexamethasone treatment (as shown by *dashed lines*) as well as the resultant hyperglycemia and hyperinsulinemia leads to the reduced hypothalamic insulin signaling, which in turn (1) reduces nutrient sensors and (2) glycogen content, (3) leads to downregulation of orexigenic neuropeptides and upregulation of anorexigenic neuropeptides, and (4) alters the neurotransmitter homeostasis. Also, there exist cross talks (as shown by *dotted lines*) among different entities such as glycogen level regulates GABA and glutamate homeostasis, which in turn regulated orexigenic neuropeptide function. Thus, this altered cascade culminates into reduced appetite in dexamethasone-treated rats

inability of AgRP/NPY to stimulate feeding. It is also supported by the fact that i.c.v. injection of GABA elicits an intense increase in food intake in rats and reciprocally i.c.v. injected GABA antagonist inhibits feeding [60]. Similar observation has been made, where central administration of glutamate [61] and glutamate receptor agonists—kainic acid, AMPK, and NMDA [62]—induced feeding, while glutamate receptor (mGlu5R) antagonist—6-methyl-2-(phenylethynyl) pyridine hydrochloride—decreased feeding [63] in rodents. Also, reduction in glycogen as seen in diabetic and stress condition, not only marks the depletion of the stored energy source but also disrupts glutamate and GABA homeostasis as proved in type 2 diabetic rodent models [64, 65]. Apart from GABA and glutamate, dopamine is other food intake-related neurotransmitters. In absence of neuronal insulin signaling, there is a rise in the dopamine-degrading enzymes such as MaoA and B, which results in increased dopamine clearance and hence reducing dopamine levels [4]. Above facts further support the present observation of decreased glutamate, GABA, and dopamine levels negatively regulating the feeding behavior.

Extrapolating the results from current model, it can be postulated that the appetite and weight loss observed during stress as well as during diabetes, is because of the multifaceted interaction of hypothalamic insulin signaling, glucocorticoid levels, appetite-regulating neuropeptides, and neurotransmitters as described in summary in Fig. 7. Thus, dexamethasone-treated model represents a promising rodent model to explore hypothalamic deregulation culminating into weight loss and dysregulated energy homestasis.

Author's Contribution SG, RC, and GK conceived and designed the study; SB and SN assisted RC in the animal experiments; JM perfomed the neurotransmitter estimation under the supervision of MRY; and RC and SG analyzed the data and wrote the manuscript.

Compliance with Ethical Standards

Conflict of Interest The authors declare that they have no conflict of interest.

References

1. Ghasemi R, Haeri A, Dargahi L, Mohamed Z, Ahmadiani A (2013) Insulin in the brain: sources, localization and functions. Mol Neurobiol 47:145–171

2. Kleinridders A, Ferris HA, Cai W, Kahn CR (2014) Insulin action in brain regulates systemic metabolism and brain function. Diabetes 63:2232–2243

3. Grillo CA, Piroli GG, Lawrence RC, Wrighten SA, Green AJ, Wilson SP, Sakai RR, Kelly SJ, et al. (2015) Hippocampal insulin resistance impairs spatial learning and synaptic plasticity. Diabetes.

4. Kleinridders A, Cai W, Cappellucci L, Ghazarian A, Collins WR, Vienberg SG, Pothos EN, Kahn CR (2015) Insulin resistance in brain alters dopamine turnover and causes behavioral disorders. Proc Natl Acad Sci U S A 112:3463–3468

5. Kullmann S, Heni M, Veit R, Scheffler K, Machann J, Haring HU, Fritsche A, Preissl H (2015) Selective insulin resistance in homeostatic and cognitive control brain areas in overweight and obese adults. Diabetes Care 38:1044–1050

6. Rafacho A, Ortsater H, Nadal A, Quesada I (2014) Glucocorticoid treatment and endocrine pancreas function: implications for glucose homeostasis, insulin resistance and diabetes. J Endocrinol 223: R49–R62

7. Park S, Jang JS, Jun DW, Hong SM (2005) Exercise enhances insulin and leptin signaling in the cerebral cortex and hypothalamus during dexamethasone-induced stress in diabetic rats. Neuroendocrinology 82:282–293

8. Juruena MF, Cleare AJ, Pariante CM (2004) The hypothalamic pituitary adrenal axis, glucocorticoid receptor function and relevance in depression. Rev Bras Psiquiatr 26:189–201

9. Garcia-Caceres C, Quarta C, Varela L, Gao Y, Gruber T, Legutko B, Jastroch M, Johansson P et al (2016) Astrocytic insulin signaling couples brain glucose uptake with nutrient availability. Cell 166: 867–880

10. Schwartz MW, Sipols AJ, Marks JL, Sanacora G, White JD, Scheurink A, Kahn SE, Baskin DG et al (1992) Inhibition of hypothalamic neuropeptide Y gene expression by insulin. Endocrinology 130:3608–3616

11. Sato I, Arima H, Ozaki N, Watanabe M, Goto M, Hayashi M, Banno R, Nagasaki H et al (2005) Insulin inhibits neuropeptide Y gene expression in the arcuate nucleus through GABAergic systems. J Neurosci 25:8657–8664

12. Zhang J (2007) The direct involvement of SirT1 in insulin-induced insulin receptor substrate-2 tyrosine phosphorylation. J Biol Chem 282:34356–34364

13. Niswender KD, Morrison CD, Clegg DJ, Olson R, Baskin DG, Myers MG Jr, Seeley RJ, Schwartz MW (2003) Insulin activation of phosphatidylinositol 3-kinase in the hypothalamic arcuate nucleus: a key mediator of insulin-induced anorexia. Diabetes 52:227–231

14. Mayer CM, Belsham DD (2009) Insulin directly regulates NPY and AgRP gene expression via the MAPK MEK/ERK signal transduction pathway in mHypoE-46 hypothalamic neurons. Mol Cell Endocrinol 307:99–108

15. Morley JE (1987) Neuropeptide regulation of appetite and weight. Endocr Rev 8:256–287

16. He J, Xu C, Kuang J, Liu Q, Jiang H, Mo L, Geng B, Xu G (2015) Thiazolidinediones attenuate lipolysis and ameliorate dexamethasone-induced insulin resistance. Metabolism 64:826–836

17. Kuo LE, Czarnecka M, Kitlinska JB, Tilan JU, Kvetnansky R, Zukowska Z (2008) Chronic stress, combined with a high-fat/high-sugar diet, shifts sympathetic signaling toward neuropeptide Y and leads to obesity and the metabolic syndrome. Ann N Y Acad Sci 1148:232–237

18. Calogero AE, Liapi C, Chrousos GP (1991) Hypothalamic and suprahypothalamic effects of prolonged treatment with dexamethasone in the rat. J Endocrinol Investig 14:277–286

19. Shimizu H, Arima H, Ozawa Y, Watanabe M, Banno R, Sugimura Y, Ozaki N, Nagasaki H et al (2010) Glucocorticoids increase NPY gene expression in the arcuate nucleus by inhibiting mTOR signaling in rat hypothalamic organotypic cultures. Peptides 31:145–149

20. Popoli M, Yan Z, McEwen BS, Sanacora G (2013) The stressed synapse: the impact of stress and glucocorticoids on glutamate transmission. Nat Rev Neurosci 13:22–37

21. Rhoads DE, DiRocco RJ, Osburn LD, Peterson NA, Raghupathy E (1984) Stimulation of synaptosomal uptake of neurotransmitter amino acids by insulin: possible role of insulin as a neuromodulator. Biochem Biophys Res Commun 119:1198–1204

22. Delgado TC (2013) Glutamate and GABA in appetite regulation. Front Endocrinol (Lausanne) 4:103

23. Meguid MM, Fetissov SO, Varma M, Sato T, Zhang L, Laviano A, Rossi-Fanelli F (2000) Hypothalamic dopamine and serotonin in the regulation of food intake. Nutrition 16:843–857

24. Kinote A, Faria JA, Roman EA, Solon C, Razolli DS, Ignacio-Souza LM, Sollon CS, Nascimento LF et al (2012) Fructose-induced hypothalamic AMPK activation stimulates hepatic PEPCK and gluconeogenesis due to increased corticosterone levels. Endocrinology 153:3633–3645

25. De Souza CT, Araujo EP, Bordin S, Ashimine R, Zollner RL, Boschero AC, Saad MJ, Velloso LA (2005) Consumption of a fat-rich diet activates a proinflammatory response and induces insulin resistance in the hypothalamus. Endocrinology 146:4192–4199

26. El-Haschimi K, Pierroz DD, Hileman SM, Bjorbaek C, Flier JS (2000) Two defects contribute to hypothalamic leptin resistance in mice with diet-induced obesity. J Clin Invest 105:1827–1832

27. Melnyk RB (1987) Decreased binding to hypothalamic insulin receptors in young genetically obese rats. Physiol Behav 40:237–241

28. Belani M, Purohit N, Pillai P, Gupta S, Gupta S (2014) Modulation of steroidogenic pathway in rat granulosa cells with subclinical Cd exposure and insulin resistance: an impact on female fertility. Biomed Res Int 2014:460251

29. Duncan M, Singh B, Wise P, Carter G, Zadeh J (1995) A simple measure of insulin resistance. Lancet 346:120–121

30. Katyare SS, Pandya JD (2005) A simplified fluorimetric method for corticosterone estimation in rat serum, tissues and mitochondria. Indian J Biochem Biophys 42:48–53

31. Silber RH, Busch RD, Oslapas R (1958) Practical procedure for estimation of corticosterone or hydrocortisone. Clin Chem 4:278–285

32. Wingerd BD, and Stein G (1988) Rat dissection manual (Johns Hopkins University Press).

33. Chiu K, Lau W, Lau H, So K-F, Chang R-C (2007) Micro-dissection of rat brain for RNA or protein extraction from specific brain region journal of visualized experiments: JoVE 7.

34. Bhattacharyya S, Khanna S, Chakrabarty K, Mahadevan A, Christopher R, Shankar SK (2009) Anti-brain autoantibodies and altered excitatory neurotransmitters in obsessive-compulsive disorder. Neuropsychopharmacology 34:2489–2496

35. Reinhoud NJ, Brouwer HJ, van Heerwaarden LM, Korte-Bouws GA (2013) Analysis of glutamate, GABA, noradrenaline, dopamine, serotonin, and metabolites using microbore UHPLC with electrochemical detection. ACS Chem Neurosci 4:888–894

36. Kilcoyne M, Gerlach JQ, Farrell MP, Bhavanandan VP, Joshi L (2011) Periodic acid-Schiff's reagent assay for carbohydrates in a microtiter plate format. Anal Biochem 416:18–26

37. Ward CW, Menting JG, Lawrence MC (2013) The insulin receptor changes conformation in unforeseen ways on ligand binding: sharpening the picture of insulin receptor activation. BioEssays 35:945–954. doi:10.1002/bies 201370111

38. Derakhshan F, Toth C (2013) Insulin and the brain. Curr Diabetes Rev 9:102–116

39. Sakoda H, Ogihara T, Anai M, Funaki M, Inukai K, Katagiri H, Fukushima Y, Onishi Y, et al (2000) Dexamethasone-induced insulin resistance in 3 T3-L1 adipocytes is due to inhibition of glucose transport rather than insulin signal transduction. Diabetes 49:1700–1708

40. Schinkel AH, Wagenaar E, van Deemter L, Mol CA, Borst P (1995) Absence of the mdr1a P-glycoprotein in mice affects tissue distribution and pharmacokinetics of dexamethasone, digoxin, and cyclosporin a. J Clin Invest 96:1698–1705

41. Miller AH, Spencer RL, Pulera M, Kang S, McEwen BS, Stein M (1992) Adrenal steroid receptor activation in rat brain and pituitary following dexamethasone: implications for the dexamethasone suppression test. Biol Psychiatry 32:850–869

42. Yin W, Gore AC (2010) The hypothalamic median eminence and its role in reproductive aging. Ann N Y Acad Sci 1204:113–122

43. Steen E, Terry BM, Rivera EJ, Cannon JL, Neely TR, Tavares R, Xu XJ, Wands JR et al (2005) Impaired insulin and insulin-like growth factor expression and signaling mechanisms in Alzheimer's disease—is this type 3 diabetes? J Alzheimers Dis 7: 63–80

44. Mastaitis JW, Wurmbach E, Cheng H, Sealfon SC, Mobbs CV (2005) Acute induction of gene expression in brain and liver by insulin-induced hypoglycemia. Diabetes 54:952–958

45. Cotero VE, Routh VH (2009) Insulin blunts the response of glucose-excited neurons in the ventrolateral-ventromedial hypothalamic nucleus to decreased glucose. Am J Physiol Endocrinol Metab 296:E1101–E1109

46. Shimizu H, Arima H, Watanabe M, Goto M, Banno R, Sato I, Ozaki N, Nagasaki H et al (2008) Glucocorticoids increase neuropeptide Y and agouti-related peptide gene expression via adenosine monophosphate-activated protein kinase signaling in the arcuate nucleus of rats. Endocrinology 149:4544–4553

47. Klockener T, Hess S, Belgardt BF, Paeger L, Verhagen LA, Husch A, Sohn JW, Hampel B et al (2011) High-fat feeding promotes obesity via insulin receptor/PI3K-dependent inhibition of SF-1 VMH neurons. Nat Neurosci 14:911–918

48. Barthel A, Okino ST, Liao J, Nakatani K, Li J, Whitlock JP Jr, Roth RA (1999) Regulation of GLUT1 gene transcription by the serine/threonine kinase Akt1. J Biol Chem 274:20281–20286

49. Chari M, Yang CS, Lam CK, Lee K, Mighiu P, Kokorovic A, Cheung GW, Lai TY et al (2011) Glucose transporter-1 in the hypothalamic glial cells mediates glucose sensing to regulate glucose production in vivo. Diabetes 60:1901–1906

50. Qi W-w, Zhong L-y, Li X-r, Li G, Liu Z-x, Hu J-f, Chen N-h (2012) Hyperglycemia induces the variations of 11-hydroxysteroid dehydrogenase type 1 and peroxisome proliferator-activated receptor—G expression in hippocampus and hypothalamus of diabetic rats. Exp Diabetes Res 2012:107130

51. Sarruf DA, Yu F, Nguyen HT, Williams DL, Printz RL, Niswender KD, Schwartz MW (2009) Expression of peroxisome proliferator-activated receptor-gamma in key neuronal subsets regulating glucose metabolism and energy homeostasis. Endocrinology 150:707–712

52. Lu M, Sarruf DA, Talukdar S, Sharma S, Li P, Bandyopadhyay G, Nalbandian S, Fan W et al (2011) Brain PPAR-gamma promotes obesity and is required for the insulin-sensitizing effect of thiazolidinediones. Nat Med 17:618–622

53. Obel LF, Muller MS, Walls AB, Sickmann HM, Bak LK, Waagepetersen HS, Schousboe A (2012) Brain glycogen-new perspectives on its metabolic function and regulation at the subcellular level. Front Neuroenergetics 4:1–15

54. Halse R, Bonavaud SM, Armstrong JL, McCormack JG, Yeaman SJ (2001) Control of glycogen synthesis by glucose, glycogen, and insulin in cultured human muscle cells. Diabetes 50:720–726

55. Krssak M, Brehm A, Bernroider E, Anderwald C, Nowotny P, Dalla Man C, Cobelli C, Cline GW et al (2004) Alterations in postprandial hepatic glycogen metabolism in type 2 diabetes. Diabetes 53:3048–3056

56. Tavoni TM, Obici S, de Castro RMA, Minguetti-Camara VC, Curi R, Bazotte RB (2013) Evaluation of liver glycogen catabolism during hypercortisolism induced by the administration of dexamethasone in rats. Pharmacol Rep 65:144–151

57. Allaman I, Pellerin L, Magistretti PJ (2004) Glucocorticoids modulate neurotransmitter-induced glycogen metabolism in cultured cortical astrocytes. J Neurochem 88:900–908

58. Tong Q, Ye CP, Jones JE, Elmquist JK, Lowell BB (2008) Synaptic release of GABA by AgRP neurons is required for normal regulation of energy balance. Nat Neurosci 11:998–1000

59. Wu Q, Boyle MP, Palmiter RD (2009) Loss of GABAergic signaling by AgRP neurons to the parabrachial nucleus leads to starvation. Cell 137:1225–1234

60. van den Pol AN (2003) Weighing the role of hypothalamic feeding neurotransmitters. Neuron 40:1059–1061

61. Stricker-Krongrad A, Beck B, Nicolas JP, Burlet C (1992) Central effects of monosodium glutamate on feeding behavior in adult long-Evans rats. Pharmacol Biochem Behav 43:881–886

62. Stanley BG, Ha LH, Spears LC, Dee MG 2nd (1993) Lateral hypothalamic injections of glutamate, kainic acid, D,L-alpha-amino-3-hydroxy-5-methyl-isoxazole propionic acid or N-methyl-D-aspartic acid rapidly elicit intense transient eating in rats. Brain Res 613:88–95

63. Fukumoto K, Chaki S (2015) Involvement of serotonergic system in the effect of a metabotropic glutamate 5 receptor antagonist in the novelty-suppressed feeding test. J Pharmacol Sci 127:57–61

64. Schousboe A, Bak LK, Sickmann HM, Sonnewald U, Waagepetersen HS (2007) Energy substrates to support glutamatergic and GABAergic synaptic function: role of glycogen, glucose and lactate. Neurotox Res 12:263–268

65. Sickmann HM, Waagepetersen HS, Schousboe A, Benie AJ, Bouman SD (2012) Brain glycogen and its role in supporting glutamate and GABA homeostasis in a type 2 diabetes rat model. Neurochem Int 60:267–275